LAWRENCE
LIVERMORE
NATIONAL
LABORATORY

LLNL-CONF-425883

Reactive Blast Waves from Composite Charges

A. L. Kuhl, H. Reichenbach, J. B. Bell, V. E. Beckner

March 17, 2010

14th International Detonation Symposium
Coeur d' Alene, OH, United States
April 11, 2010 through April 16, 2010

Disclaimer

Reactive Blast Waves from Composite Charges

Allen L. Kuhl[*], Heinz Reichenbach[**], John B. Bell[f] and Vincent E. Beckner[f]

[*] Lawrence Livermore National Laboratory
7000 East Ave, Livermore, CA, USA 94551

[**] Director Emeritus, Ernst Mach Institut
Eckersraße 4, 79104 Freiburg, Germany

[f] Lawrence Berkeley National Laboratory
1 Cyclotron Rd, Berkeley, CA, USA 94720

Abstract. Investigated here is the performance of composite explosives—measured in terms of the blast wave they drive into the surrounding environment. The composite charge configuration studied here was a spherical PETN booster (1/3 charge mass), surrounded by exothermic powder (2/3 charge mass) at an initial density of 0.6 g/cc. The powder acts as a fuel but does not detonate—thereby providing an extreme example of a "non-ideal" explosive. The following powders were tested: flake Aluminum (Al), fine-grained TNT and PETN, sugar, polyethylene granules, and activated charcoal (d<32μm). Detonation of the booster charge creates a blast wave that disperses the powder and ignites the ensuing fuel-air mixture—thereby forming a two-phase combustion cloud embedded in the explosion. Afterburning of the booster detonation products with air also enhances and promotes the fuel-air combustion process. Pressure waves from such reactive blast waves have been measured in 3 bomb calorimeters (6.6, 21 and 40 liter chambers) and one tunnel (4 liters). Pressure histories for composite charge explosions in air were much larger than those measured in a nitrogen atmosphere—thereby demonstrating that a reactive blast wave was formed. The biggest effect was found for Al, TNT and PETN powders. A Heterogeneous Continuum Model was used to model the dispersion and combustion of the particle cloud. The model equations were integrated by high-order Godunov schemes for both the gas and particle phases. Adaptive Mesh Refinement (AMR) was used to capture the energy-bearing scales of the turbulent flow on the computational grid, and to track/resolve reaction zones. Numerical simulations of the explosion fields from 1.5-g Al-composite charges were performed. Computed pressure histories were similar to the measured waveforms, thereby validating the model.

Introduction

Investigated here is the performance of composite explosives—measured in terms of the blast wave they drive into the surrounding environment. The composite charge configuration studied here was a spherical PETN booster (1/3 charge mass), surrounded by aluminum (Al)

powder (2/3 charge mass) at an initial density of 0.6 g/cc. The Al powder acts as a fuel but does not detonate—thereby providing an extreme example of a "non-ideal" explosive. Detonation of the booster charge creates a blast wave that disperses the Al powder and ignites the ensuing Al-air mixture—thereby forming a two-phase combustion cloud embedded in the explosion. Afterburning of the booster detonation products with air also enhances and promotes the Al-air combustion process. Pressure waves from such reactive blast waves have been measured in bomb calorimeter experiments[1],[2]. In the next section we give an over-view of those experiments, and present pressure waveforms measured in three chambers (6.6, 21 and 40 liters) and one calorimetric tunnel (4 liters). In the subsequent section we describe a Heterogeneous Continuum Model[3] that was used to model the dispersion and combustion of the Al particle cloud. Computed waveforms are compared with measurements to assess the validity of the model. This is followed by conclusions.

Experiments

Experiments were conducted in three cylindrical calorimeters: **A** (L = 21 cm, D = 20 cm, V = 6.6 l), **B** (L = 30 cm, D = 30 cm, V = 21.2 l), and **C** (L = 37.9 cm, D = 36.9 cm, V = 40.5 l) and a rectangular tunnel **D** (L = 38.6 cm, X=Y = 10.1 cm, V = 3.98 l).

The composite charge construction is shown in Fig. 1. It begins with a 0.5-g spherical PETN booster (initial density of 1 g/cc). The booster is surrounded by a thin paper cylinder, and the void space (~ 1.6 cm^3) is filled with 1 g of flake Aluminum (with a bulk density of 0.63 g/cc). SEM photographs of the Al powder indicate a flake-like structure of characteristic lateral dimension 100 microns and a thickness of 1 micron (Fig. 2). According to the manufacturer (Merk, AG), the Al content of the powder was more than 93% by mass. The booster was detonated by an exploding bridge wire located at the charge center. Detonation of the booster created an expanding fuel cloud of explosion products gases and hot aluminum particles. When this fuel mixed with air, it formed a turbulent combustion cloud that consumed the aluminum and liberated 31 kJ/g of energy in addition to the energy of the booster that created the explosion.

The main diagnostic consisted of 8 piezo-electric crystal pressure gages (Kistler 603B); their fast response was needed to capture the shock front details. Flame temperatures of 4,000 K are possible for Al-air combustion cases; to eliminate thermal effects piezo-resistive gauges (Kistler 4075A) were also used. Gauges were mounted in the lid of the calorimeter or roof of the tunnel. Gauge locations, Slant Ranges (SL) from the charge center and angle α from the normal to the reflecting plane are listed in the Appendix.

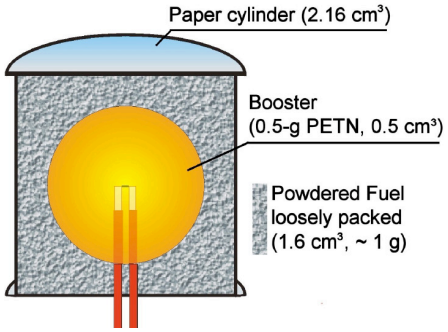

Fig. 1. Schematic of the 1.5-g composite charge.

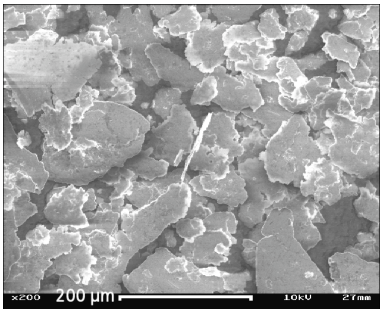

Fig. 2. SEM photograph of the flake Aluminum powder (Merck, AG).

Pressure histories created by composite charge explosions in chambers **A**-**D** are presented in Figs. 3-6. Pressure histories for explosions in air are considerably larger than those in nitrogen—thereby proving the existence of a reactive blast wave for this composite charge configuration.

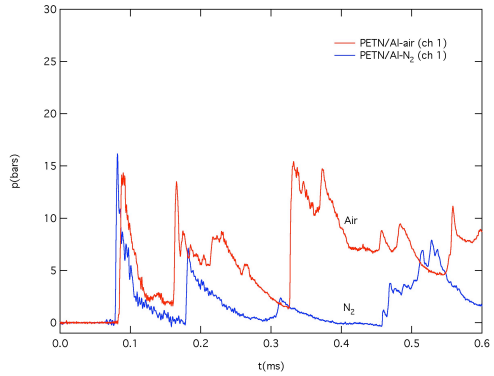

Fig. 3. Reflected pressure histories measured on the lid of chamber **A** for 1.5-g composite charges detonated in air and N_2 (*SR* = 11.6 cm, α =26 deg).

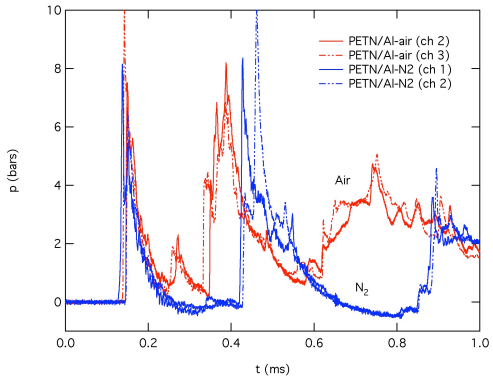

Fig. 4. Reflected pressure histories measured on the lid of chamber **B** for 1.5-g composite charges detonated in air and N_2 (*SR* = 15.8 cm, α =18 deg).

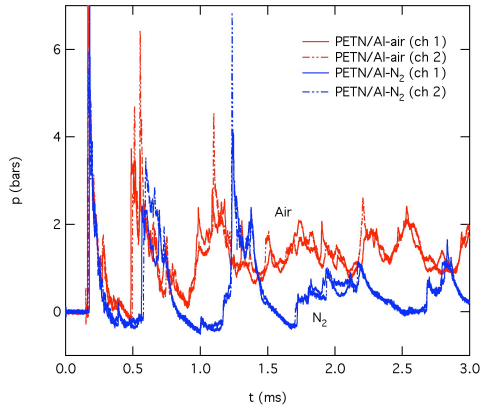

Fig. 5. Reflected pressure histories measured on the lid of chamber **C** for 1.5-g composite charges detonated in air and N_2 (*SR* = 19 cm, α = 15 deg).

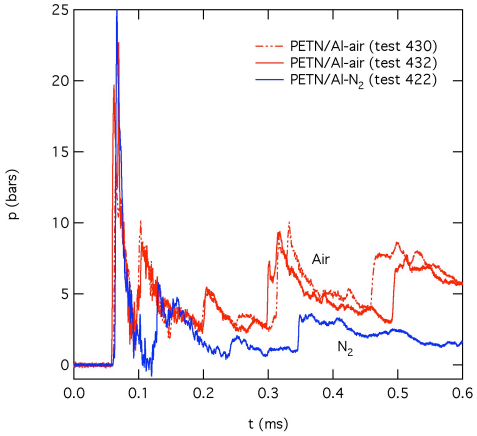

Fig. 6. Reflected pressure histories measured on the lid of tunnel **D** for 1.5-g composite charges detonated in air and N_2 (*SR* = 9 cm, α = 56 deg).

Particle Size Effects

Experiments were conducted with aluminum powders of different particle-size distributions. Starting from a single batch of powder, the powder was sieved to allow particles smaller than d_i (125 μm, 50 μm and 25 μm) to pass through the filter. SEM photographs of the resulting three powders are shown in Fig. 7.

Experiments were conducted in chamber **B**; pressure histories measured at channel 2 on the chamber lid are shown in Fig. 8. All waveforms are enhanced, compared to the test performed in nitrogen, thereby showing the reactive blast wave effect. The first and second blast waves for the flake Al composite charge arrived ahead of the waveforms for the Al powders, indicating faster energy release for the flake Al. Waveforms for the Al powder charges were qualitatively similar—probably because the finest particles burn first—and all powders had similar fine particles (due to the sieving process).

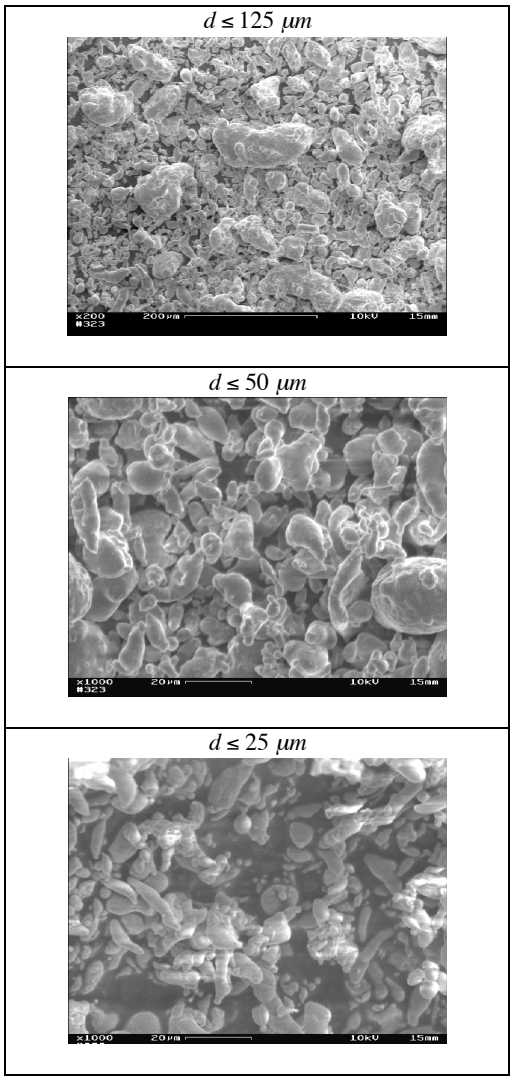

Figure 7. SEM photographs of an aluminum powders, filtered with sieves allowing particles smaller than d to pass through the filter.

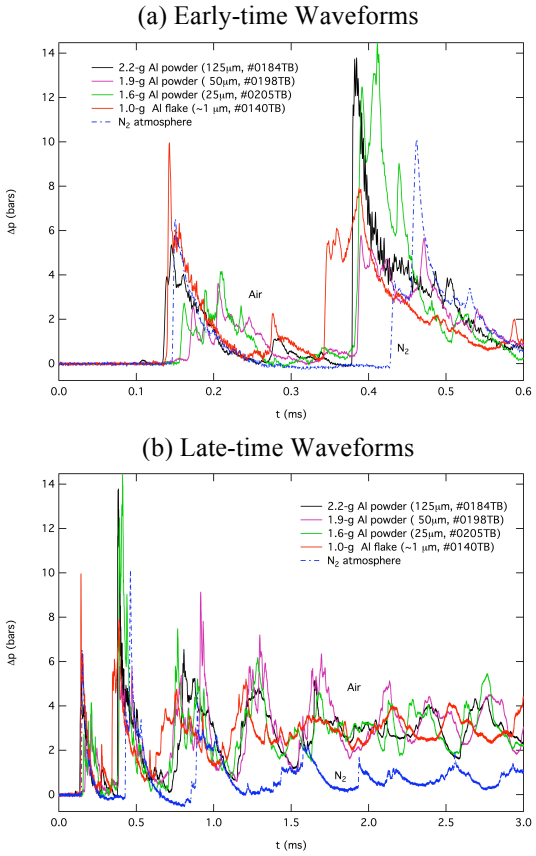

Figure 8. Blast wave dependence on particle size: chamber **B**, composite charges detonated in air and N_2 (SR = 15.8 cm, α=18 deg).

Other Powder Fuels

We have also investigated reactive blast waves from other composite fuel charges. The Al fuel in composite charge (Fig. 1) was replaced by ~1-g of reactive (but non-detonating) powder, such as: TNT powder, PETN powder, confectioners sugar ($C_{12}H_{22}O_{11}$), polyethylene PE = $(C_2H_4)_n$ granules, or activated charcoal powder (d < 32 μm). Reactive blast waves measured from powder fuel composite charges are presented in Figs. 9, 10 and 11. The biggest reactive effects were found for Al, TNT, and PETN powders, and confectioners sugar; PE and charcoal powders gave little effect. Note that TNT powder gave more effect than a TNT solid charge (e.g., late time pressures were similar to the Al powder composite charge).

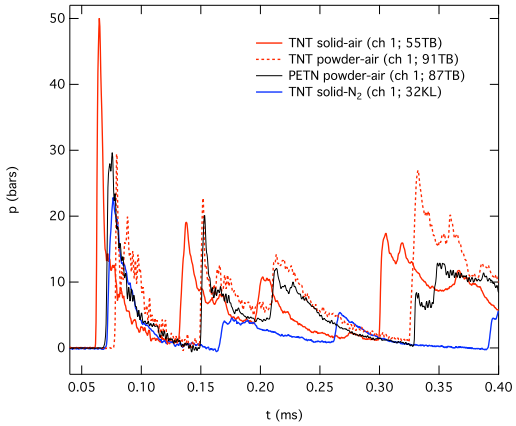

Figure 9. Blast waves measured from TNT-solid, TNT-powder and PETN-powder composite charges in air and nitrogen (chamber A).

(a) Early-time Waveforms

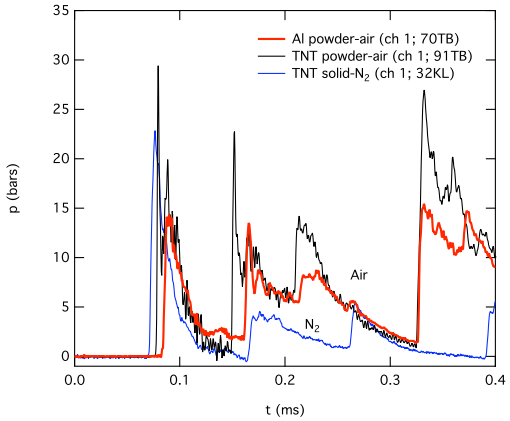

(b) Late-time Waveforms

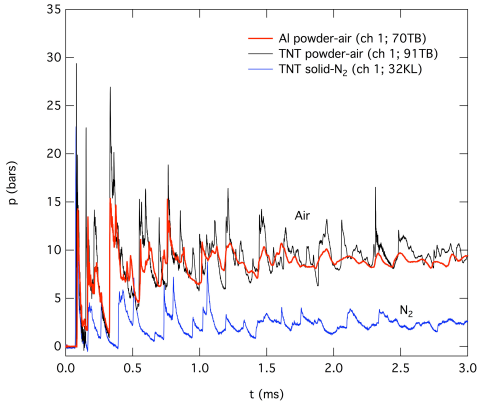

Figure 10. Blast waves measured from Al and TNT powder composite charges detonated in air and nitrogen (chamber **A**).

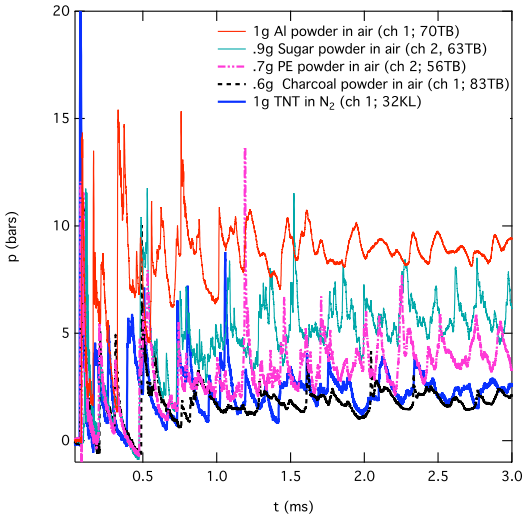

Figure 11. Blast waves measured from other powder fuel (sugar, PE, charcoal) composite charges are compared with Al powder (chamber **A**).

Height-of-Burst Experiments

The 1.5-gram composite charge design was scaled up to 3 kg and 10 kg, corresponding to energy-per-unit-volume loadings of chambers **B** and **A**, respectively. A SEM photograph of the powder is provided in Fig. 12; it has the appearance of "corn flakes."

The charges were detonated at 122 cm above a reflecting plane (Height of Burst: *HOB* = 122 cm). A pressure gauge located directly bellow the charge (*GR*=0), measured the reflected blast wave history. Results are shown in Figs. 13 and 14, and compared to the blast wave from the booster charge alone. Comparison of the two measurements shows that the reactive blast wave effect is considerably stronger at larger scales.

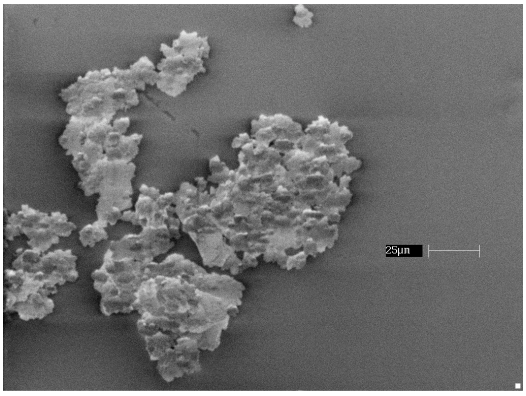

Fig. 12. SEM photographs of the flake Aluminum powder (bar scale = 25 μm).

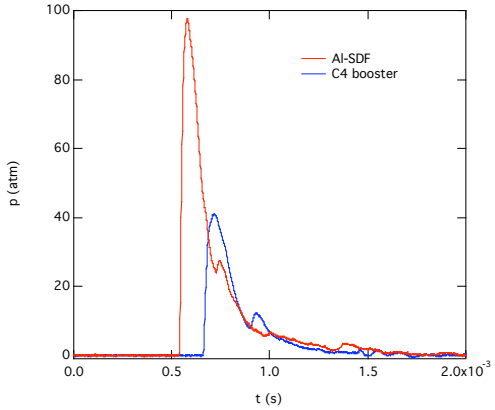

Fig. 13. Reflected pressure history from a 3-kg composite charge at *HOB* = 122 cm (*GR* = 0).

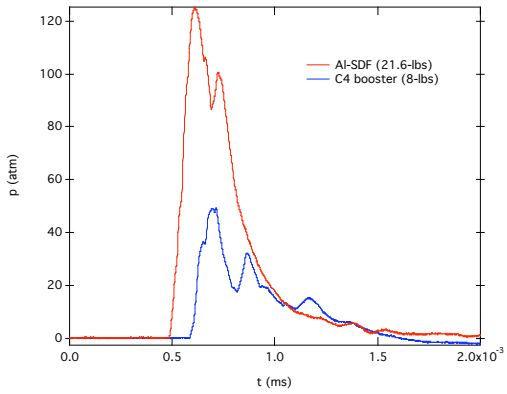

Fig. 14. Reflected pressure history from a 10-kg composite charge at *HOB* = 122 cm (*GR* = 0).

Heterogeneous Continuum Model

The model is based on the Eulerian multi-phase conservation laws for a dilute heterogeneous continuum as formulated by Nigmatulin[9]. We model the evolution of the gas phase combustion fields in the limit of large Reynolds and Peclet numbers, where effects of molecular diffusion and heat conduction are negligible on the gasdynamic fields. The flow field is governed by the following conservation laws:

$$\partial_t \rho + \nabla \cdot (\rho \mathbf{u}) = \dot{\sigma}_s \quad (1)$$

$$\partial_t \rho \mathbf{u} + \nabla \cdot (\rho \mathbf{u}\mathbf{u} + p) = \dot{\sigma}_s \mathbf{v} - \dot{f}_s \quad (2)$$

$$\partial_t \rho E + \nabla \cdot (\rho \mathbf{u} E + p\mathbf{u}) = -\dot{q}_s + \dot{\sigma}_s E_s - \dot{f}_s \cdot \mathbf{v} \quad (3)$$

where ρ, p, u represent the gas density, pressure and specific internal energy, $\mathbf{u}$ is the gas velocity vector, and $E \equiv u + \mathbf{u} \cdot \mathbf{u}/2$ denotes the total energy of the gas phase. Source terms on the right hand side take into account: mass transfer from the particle phase to gas phase ($\dot{\sigma}_s$), acceleration of particle phase by drag ($\dot{f}_s$), and heat exchange ($\dot{q}_s$) to the particle phase.

We treat the particle phase as an Eulerian continuum field. We consider the dilute limit, devoid of particle-particle interactions, so that the pressure and sound speed of the particle phase are zero. We model the evolution of particle phase mass, momentum and energy fields by the conservation laws of continuum mechanics for heterogeneous media[9]:

$$\partial_t \sigma + \nabla \cdot \sigma \mathbf{v} = -\dot{\sigma}_s \quad (4)$$

$$\partial_t \sigma \mathbf{v} + \nabla \cdot \sigma \mathbf{v}\mathbf{v} = -\dot{\sigma}_s \mathbf{v} + \dot{f}_s \quad (5)$$

$$\partial_t \sigma e_s + \nabla \cdot \sigma e_s \mathbf{v} = \dot{q}_s - \dot{\sigma}_s e_s \quad (6)$$

where σ and $\mathbf{v}$ represent the particle-phase density and velocity, and $e_s \equiv C_s T_s$ denotes the specific internal energy of the particle phase.

We consider two fuels: PETN detonation products (F_1) and Aluminum (F_2), along with their corresponding combustion products: PETN-air (P_1) and Al-air (P_2). We model the global

combustion of both fuels F_k with air (A) producing equilibrium combustion products P_k:

$$F_k + A \Rightarrow P_k \qquad (k = 1 \text{ or } 2) \tag{7}$$

The mass fractions Y_k of the components are governed by the component conservation laws:

$$\partial_t \rho Y_{Fk} + \nabla \cdot \rho Y_{Fk} \mathbf{u} = -\dot{s}_k + \delta_{k2} \dot{\sigma}_k \tag{8}$$

$$\partial_t \rho Y_A + \nabla \cdot \rho Y_A \mathbf{u} = -\sum_k \alpha_k \dot{s}_k \tag{9}$$

$$\partial_t \rho Y_{Pk} + \nabla \cdot \rho Y_{Pk} \mathbf{u} = \sum_k (1 + \alpha_k) \dot{s}_k \tag{10}$$

Fuel and air are consumed in stoichiometric proportions: $\alpha_k = A / F_k$. In the above, $\dot{s}_k$ represents the global kinetics sink term. In this work we use the fast-chemistry limit that is consistent with the inviscid gasdynamic model (1)-(3), so whenever fuel and air enter a computational cell, they are consumed in one time step. The term $\delta_{k2} \dot{\sigma}_k$ represents the conversion of Al from the particle phase to the gas phase, which creates a source of Al fuel.

More details of the Model (e.g., inter-phase interaction terms and Equations of State), a description of the high-order Godunov schemes used to integrate the above conservation laws, as well as the Adaptive Mesh Refinement (AMR) method used to capture the turbulent mixing scales on the mesh can be found in our publications.[3, 4]

Numerical Simulations

Our 3-d two-phase AMR code was used to simulate the explosion of a 1.5-g composite charge in chamber **B**. A vertical cross-sectional view of the temperature field at different times is depicted in Fig. 15. The booster detonation products push the Al fuel into a thin shell (28 μs); by 55 μs combustion is occurring along the mixing fingers; by 100 μs turbulent mixing has distributed combustion throughout the chamber.

The computed pressure is compared with the experimental measurements in Fig. 16. The AMR simulation (*red curve*), employing an ignition temperature model, compares favorably to three pressure records (channels 2, 3 and 4) measured on the same experiment in air. A comparision of these with the experiment in N_2 (*blue curve*) clearly shows the reactive blast wave effect induced by Al particle combustion with air.

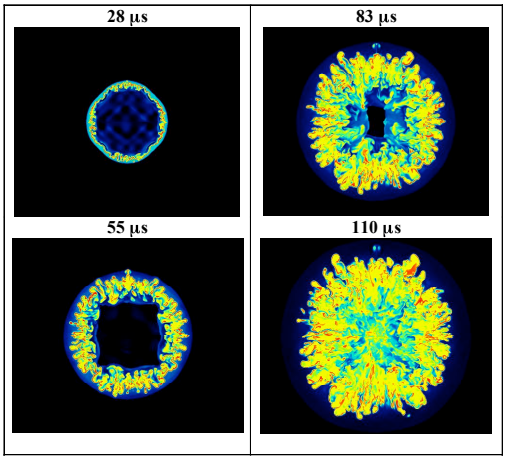

Fig. 15. Vertical cross-section views of the temperature field in chamber **B**, created by the explosion of a 1.5-g composite charge in air (*blue*=300K, *green*=2,000K, *yellow*=3,000K, *red*=4,000K).

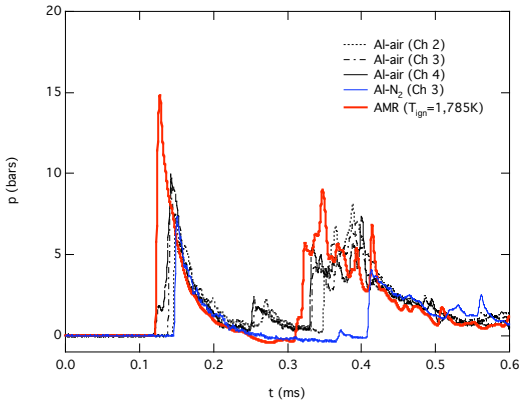

Fig. 16. Reflected pressure histories of the reactive blast wave from a 1.5-g composite charge measured on the lid of chamber **B** (*black curves* = experiment in air, *red curve* = AMR simulation, *blue curve* = experiment in N_2).

Conclusions

Blast waves from "non-ideal" explosive charges have been studied experimentally and theoretically, via numerical simulations with our two-phase AMR code. Experiments with 1.5 g composite charges in air and N_2 demonstrate the existence of a reactive blast wave created by the turbulent combustion of the particles with air. This combustion region is able to keep up with the shock due to the initial ballistic mixing of the particles induced by the blast wave of the booster charge. According to the experiments, this effect is largest for Al, TNT and PETN powders.

The reactive blast wave effect is even more enhanced at larger scales. Unconfined blast waves from 3-kg and 10-kg Al powder composite charges detonated at a *HOB* = 122 cm from a reflecting plane were also measured. Pressure histories and impulses were 2.5 times larger than those from the booster charge alone. Again, we attribute this to a ballistic mixing effect inherent in the charge design (Fig. 1). Field tests with even larger charges (say 100-kg charges) should be performed to further investigate such scaling issues.

Reflected pressure histories from our AMR code simulations were similar to measured waveforms—thereby proving that our hetero-geneous continuum model captures the dominant features of this two-phase combustion flow.

Acknowledgements

This work performed under the auspices of the U.S. Department of Energy by Lawrence Livermore National Laboratory under Contract DE-AC52-07NA27344. **LLNL-CONF-418406**

References

1. Kuhl, A. L., and Reichenbach, H., "Combustion Effects in Confined Explosions" *Proceedings of the Combustion Institute* Vol. 32, pp. 2291-2298, 2009.

2. Kuhl, A. L. & Reichenbach, H., Barometric Calorimeters, *ХИМИЧЕСКАЯ ФИЗИКА, том 29, № 3, с. 1–8*, 2010.

3. Kuhl, A. L., Bell, J. B. & Beckner, V. E., "Heterogeneous Continuum Model of Aluminum Particle Combustion in Explosions", *Fizika Goreniya I Vzryva*, Vol. 4 (in press) 2010.

4. Kuhl, A. L., Bell, J. B., Beckner, V. E., and Khasainov, B., "Numerical Simulations of Thermobaric Explosions", *Energetic Materials: Characterization and Performance of Advanced Systems, 38th Int. Annual Conf. of ICT*, Fraunhofer Inst. Chemicsch Technologie, Pfinztal, pp. 1.1-14, 2007.

5. Kuhl, A. L, Bell, J. B. and Beckner, V. E., "Gasdynamic Model of Turbulent Combustion in TNT Explosions", *33rd International Combustion Symposium*, 2010.

6. Nigmatulin, R. I., *Dynamics of Multi-phase Flows,* Vol. 1, 464 pp., Nauka, Moscow, 1987.

Appendix

Locations of the pressure gauges

Case	*HOB* (cm)	*GR* (cm)	*SR* (cm)	α (deg)
Chamber **A**	10.5	5	11.6	25.5
Chamber **B**	15	5	15.8	18.4
Chamber **C**	19	5	19.6	14.8
Tunnel **D**	5	7.5	9	56.3

HOB ≡ Height of Burst

GR ≡ Ground Range

$SR \equiv \text{Slant Range} = \sqrt{HOB^2 + GR^2}$

$\alpha = Tan^{-1}(GR/HOB)$